Viroporin activity of the JC polyomavirus is regulated by interactions with the adaptor protein complex 3

Tadaki Suzuki[a,b], Yasuko Orba[a], Yoshinori Makino[a], Yuki Okada[c], Yuji Sunden[d], Hideki Hasegawa[b,e], William W. Hall[e,f], and Hirofumi Sawa[a,e,g,1]

[a]Division of Molecular Pathobiology, Research Center for Zoonosis Control, Hokkaido University, Sapporo 001-0020, Japan; [b]Department of Pathology, National Institute of Infectious Diseases, Musashimurayama 208-0011, Japan; [c]Laboratory of Molecular Cellular Pathology, Hokkaido University School of Medicine, Sapporo 060-8638, Japan; [d]Laboratory of Comparative Pathology, Hokkaido University School of Veterinary Medicine, Sapporo 060-0818, Japan; [e]Global Virus Network, Baltimore, MD 21201; [f]Centre for Research in Infectious Diseases, University College Dublin, Dublin 4, Ireland; and [g]Global Centers of Excellence Program for Zoonosis Control, Hokkaido University, Sapporo 001-0020, Japan

Edited* by Robert C. Gallo, Institute of Human Virology, University of Maryland School of Medicine, Baltimore, MD, and approved October 3, 2013 (received for review June 20, 2013)

Viroporins, which are encoded by a wide range of animal viruses, oligomerize in host cell membranes and form hydrophilic pores that can disrupt a number of physiological properties of the cell. Little is known about the relationship between host cell proteins and viroporin activity. The human JC polyomavirus (JCV) is the causative agent of progressive multifocal leukoencephalopathy. The JCV-encoded agnoprotein, which is essential for viral replication, has been shown to act as a viroporin. Here we demonstrate that the JCV agnoprotein specifically interacts with adaptor protein complex 3 through its δ subunit. This interaction interrupts adaptor protein complex 3–mediated vesicular trafficking with suppression of the targeting of the protein to the lysosomal degradation pathway and instead permits the transport of agnoprotein to the cell surface with resulting membrane permeabilization. The findings demonstrate a previously undescribed paradigm in virus–host interactions allowing the host to regulate viroporin activity and suggest that the viroporins of other viruses may also be highly regulated by specific interactions with host cell proteins.

pathogen–host cell interaction | intracellular vesicular trafficking

JC polyomavirus (JCV) is a member of the family of polyomaviruses and the etiologic agent of progressive multifocal leukoencephalopathy, a neurological disorder associated with destructive infection of oligodendrocytes (1). The genome of JCV consists of three functional regions: an early coding region, a late coding region, and a transcriptional control region. The early coding region encodes the large and small T antigens, and the late coding region encodes VP1, VP2, VP3, and agnoprotein (2).

Recently, we have shown that JCV agnoprotein acts as a viroporin and promotes virus replication by increasing membrane permeabilization, which facilitates the release of progeny virions. Mutational analysis of the agnoprotein has demonstrated that the amino acids Arg8 and Lys9 in the NH_2 terminus are critical because mutation of these RK residues (RK8AA mutant) abrogates viroporin function (3). Viroporins are small, nonglycosylated, highly hydrophobic viral polypeptides which interact with cell membranes and increase their permeability to ions and other low-molecular weight molecules (4–6). Upon membrane insertion, viroporins oligomerize to create hydrophilic pores (7–11); although some viroporins are not required for production of viral progeny, their expression can significantly increase the formation of new virus particles (12–15).

Notably, some viroporins have also been shown to influence intracellular protein trafficking. Poliovirus 3A can inhibit endoplasmic reticulum (ER)-to-Golgi transit, resulting in the shutoff of nascent MHC class I/peptide complex trafficking and the down-regulation of cytokine secretion (16, 17). Coxsackievirus 2B, 2BC, and 3A viroporins are capable of blocking trafficking through the Golgi complex (18, 19). Thus, although intracellular trafficking of proteins is important in viral infection, the relation between viroporin activity and cellular trafficking processes remains poorly understood.

In the present study, we have investigated the role of cellular proteins in the viroporin activity of the JCV agnoprotein. We demonstrated an interaction of the agnoprotein with the δ subunit of adaptor protein complex 3 (AP-3) (AP3D) and showed that this interaction prevents AP-3–mediated vesicular trafficking and blocks the targeted transport of the agnoprotein for lysosomal degradation. Ultimately, this results in the transport of agnoprotein to the cell surface, thus facilitating viroporin activity.

Results

Agnoprotein Impairs AP-3–Mediated Intracellular Vesicular Trafficking. To investigate if host protein(s) are associated with the viroporin activity of agnoprotein, we performed a yeast two-hybrid screen using the N-terminal 24 amino acid (a.a.) residues as bait, which included the RK residues. Among 29 clones, 7 clones encoding partial sequences of AP3D were identified, and the shortest fragment among these encoded the 548–850 a.a. residues of AP3D isoform 2 (Fig. 1*A*). The agnoprotein–AP3D interaction was confirmed using several GST-AP3D recombinant proteins (AP3D-Y27, AP3D-Y27N, and AP3D-Y27C) produced in *Escherichia coli*. No interactions were seen with agnoprotein with GST alone or with GST-AP3D-Y27N. In contrast, interactions were seen with GST-AP3D-Y27 and GST-AP3D-Y27C (Fig. 1*B* and Fig. S1*A*), suggesting that the C-terminal 206 a.a. of the AP3D hinge region is important in WT binding but not the RK8AA mutant. The interaction was also confirmed in mammalian cells using immunoprecipitation methods (Fig. 1 *C* and *D*). GST pull-down assays using the minimum binding site of AP3D (AP3D-

Significance

Viroporins are small, hydrophobic viral proteins that form pores on host cell membranes, and their expression can increase the production of progeny virus particles. Recently, we have shown that human JC polyomavirus agnoprotein acts as a viroporin. We have investigated the role of host cellular proteins in the viroporin activity of the agnoprotein. We demonstrated that an interaction of the agnoprotein with the δ subunit of AP-3 prevents AP-3–mediated vesicular trafficking and blocks the targeted transport of the agnoprotein for lysosomal degradation. These findings demonstrate a previously undescribed paradigm in virus–host interactions regulating virus replication and suggest that viroporins of other viruses may also be regulated by specific interactions with host cellular proteins.

Author contributions: T.S., W.W.H., and H.S. designed research; T.S., Y. Orba, Y.M., Y. Okada, Y.S., H.H., and H.S. performed research; T.S., Y. Orba, Y.M., Y. Okada, and Y.S. contributed new reagents/analytic tools; T.S., Y. Orba, Y.M., and Y. Okada analyzed data; and T.S., W.W.H., and H.S. wrote the paper.

The authors declare no conflict of interest.

*This Direct Submission article had a prearranged editor.

[1]To whom correspondence should be addressed. E-mail: h-sawa@czc.hokudai.ac.jp.

This article contains supporting information online at www.pnas.org/lookup/suppl/doi:10.1073/pnas.1311457110/-/DCSupplemental.

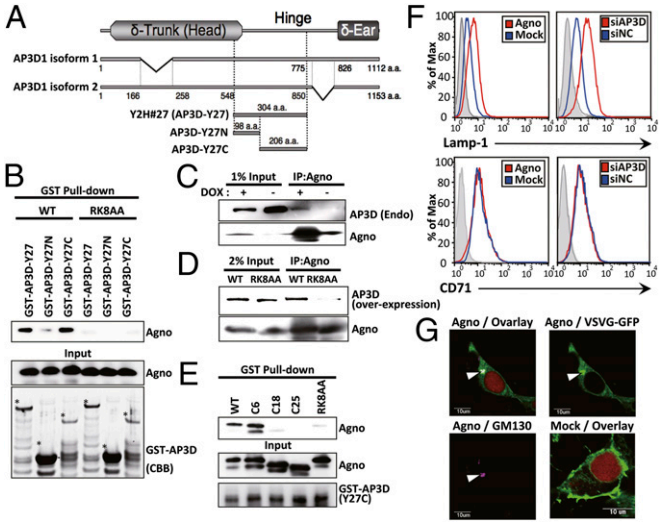

Fig. 1. Agnoprotein binds to AP3D and impairs AP-3–mediated vesicular trafficking. (*A*) Schematic representation of the δ subunit of the human AP-3 complex (AP3D1 isoforms 1 and 2), showing the region encoded by the shortest cDNA fragments (Y2H#27) isolated using a yeast two-hybrid assay and the fragments expressed as GST fused proteins (AP3D-Y27, AP3D-Y27N, and AP3D-Y27C). (*B*) GST pull-down assay with the GST fused proteins. After incubation with cellular lysates transfected with pCMV-Agno or pCMV-RK8AA, the GST fusion proteins were precipitated with glutathione-Sepharose and bound proteins were subjected to immunoblot analysis with anti-agnoprotein Ab (*Top*). The aliquots from lysates applied to the pull-down experiments were also subjected to immunoblot analysis with anti-agnoprotein antibody (*Middle*). GST fusion proteins were subjected to coomassie brilliant blue (CBB) staining (*Bottom*). Asterisks indicate the mature recombinant proteins. (*C*) Cellular lysates from agnoprotein-inducible [DOX (+)] 293AG cells were subjected to immunoprecipitation with anti-agnoprotein Ab (IP:Agno), followed by immunoblotting with anti-AP3D and anti-agnoprotein antibodies. (*D*) 293AG (WT) or 293RK8AA (RK8AA) cells were transfected with pCMV-mycAP3D and incubated in the presence of DOX. Cellular lysates were subjected to immunoprecipitation with anti-agnoprotein Ab (IP:Agno), followed by immunoblotting with the indicated antibodies. (*E*) GST pull-down assay with the GST-AP3D-Y27C and in vitro synthesized agnoprotein deletion mutant (C6, C18, and C25). After incubation with in vitro synthesized agnoprotein, the GST fusion proteins were precipitated with glutathione-Sepharose and bead-bound proteins were subjected to immunoblot analysis with anti-agnoprotein Ab (*Top*). The aliquots from mixtures before pull-down experiment were also subjected to immunoblot analysis with anti-agnoprotein (*Middle*) or GST (*Bottom*) antibody. (*F*) Levels of lysosomal membrane protein (Lamp-1) and CD71 on the cell surface were quantified by flow cytometry. (*G*) The 293T cells were transfected with pVSVG-GFP, pERedNLS-Agno (Agno), or pERedNLS (Mock) for evaluation of VSVG-GFP transport to the plasma membrane. VSVG-GFP accumulated in the perinuclear region and colocalized with the TGN marker, GM130 (arrowheads). Red represents DSRed expression in nuclei as a marker of transfection.

Y27C) and in vitro synthesized agnoprotein deletion mutants [C6, C18, and C25; deletion of 5, 17, and 24 a.a. in the N-terminal region of agnoprotein, respectively (Fig. S1*B*)] demonstrated that the N-terminal 12 a.a. (6–17) including RK residues of agnoprotein is involved in AP3D binding (Fig. 1*E*).

We carried out similar studies on the BK polyomavirus (BKV) agnoprotein, another member of the polyomavirus family. The BKV agnoprotein differs from JCV in that it has a Gln-9 instead of Lys-9, and we found that there was no interaction with AP3D. Specifically, GST pull-down assays using in vitro synthesized WT and the K9Q mutant JCV agnoprotein and BKV agnoprotein (Fig. S1*C*) demonstrated that lysine residues at position 9 (Lys-9) of JCV agnoprotein are critical for AP3D binding (Fig. S1*D*). The interaction between JCV agnoprotein and AP3D did not occur with the K9Q mutant of the JCV agnoprotein or with the BKV agnoprotein which has Gln-9 instead of Lys-9 (Fig. S1*E*).

AP3D is involved in the biogenesis of lysosome-related organelles (20). We investigated if agnoprotein could modify AP-3–mediated intracellular trafficking. In AP-3 complex-deficient mammalian cells, some lysosomal membrane proteins, including Lamp-1, exhibit increased trafficking to the plasma membrane, although their steady-state distribution is still primarily lysosomal (20, 21). We examined the status of both lysosomal (Lamp-1) and nonlysosomal (CD71) integral membrane proteins by flow cytometry. Lamp-1 expression was increased on the surface of the cells transfected with agnoprotein or an AP3D-targeted siRNA compared with cells transfected with mock plasmid or a negative control siRNA. In contrast, cell surface expression levels of CD71 were unchanged (Fig. 1*F*).

Previous studies have shown that the transport of vesicular stomatitis virus G protein (VSVG) from the trans-Golgi network (TGN) to the cell surface requires AP3D (22). The 293T cells were transfected with plasmids encoding VSVG-GFP and agnoprotein and examined by confocal microscopy. In the absence of agnoprotein, VSVG-GFP was transported to the plasma membrane and was only minimally detected in the perinuclear region at 180 min. However, in the presence of agnoprotein, the VSVG-GFP signal in the perinuclear region, which colocalized with the TGN marker protein (GM130), was still evident at 180 min (Fig. 1*G* and Fig. S2 *A* and *B*), suggesting that transport from the TGN to the cell surface was inhibited by agnoprotein. The transport of VSVG-GFP between the ER and the TGN, which is independent of AP3D, was not disrupted by agnoprotein (Fig. S2*C*). The inhibition of VSVG-GFP transport by agnoprotein could be rescued by overexpression of AP3D (Fig. S3 *A*–*C*) and was also enhanced following inhibition of AP3D expression by siRNA knockdown (Fig. S3 *D* and *E*). These observations clearly demonstrate that agnoprotein inhibited AP-3–mediated transport of VSVG-GFP from the TGN to the plasma membrane.

Disruption of the AP-3 Pathway by the Agnoprotein–AP3D Interaction is Necessary for Agnoprotein Viroporin Activity. To further investigate the interaction of agnoprotein with AP3D on viroporin function, we performed Hygromycin B (HygB, a general inhibitor of translation) membrane permeability assays (3) with Doxycycline (DOX)-inducible WT agnoprotein (SVG-AG) and RK8AA mutant (SVG-RK8AA; Arg-8 and Lys-9 of agnoprotein substituted by Ala and no viroporin activity) cells. In SVG-AG cells, the amount of agnoprotein induced by 1 μg/mL of DOX treatment was similar to that of JCV-infected parent SVG-A cells (Fig. S4 *A* and *B*). SVG-AG and SVG-RK8AA cells were incubated with or without DOX for 72 h. Nascent protein synthesis in cells with HygB was quantified by labeling newly synthesized proteins with Alexa Fluor 488. In SVG-AG cells, DOX treatment-induced agnoprotein expression and the amount of newly synthesized protein were decreased in the presence of HygB compared with its absence. In contrast, the levels of nascent protein synthesis were relatively unaltered in SVG-RK8AA cells (Fig. 2*A* and Fig. S5*A*). To demonstrate the importance of the interaction between agnoprotein and AP3D on membrane permeabilization, we established SVG-AG cells stably expressing partial fragments of AP3D, including Y27N, which does not bind agnoprotein, or Y27C, which can bind, and then performed the HygB membrane permeability assays. Newly synthesized proteins were detected in the cells expressing Y27C and WT agnoprotein. In contrast, protein synthesis was markedly decreased in the cells expressing Y27N or Mock with WT agnoprotein (Fig. 2*B* and Fig. S5*B*). These results suggested that the AP3D mutant, Y27C, interacted with agnoprotein leading to an inhibition of agnoprotein-induced membrane permeabilization.

To obtain direct evidence of agnoprotein-induced membrane permeabilization, cells were stained with a lipophilic dye (FM1-43FX). In the absence of agnoprotein, only a minimal amount of dye was detected at the intracellular membranes. In contrast, FM1-43FX dye flowed into cells in the presence of agnoprotein (Fig. S5*C*). RK8AA failed to enhance membrane permeability (Fig. 2*C* and Fig. S5*D*). Y27C inhibited agnoprotein-induced

membrane permeabilization for FM1-43FX in a manner similar to HygB (Fig. 2*D* and Fig. S5*E*).

To further evaluate the interaction between agnoprotein and AP3D, we performed JCV growth assays. After inoculation of JCV into SVG-A cells expressing Y27N or Y27C, the amount of VP1 in the culture supernatant from cells expressing the latter was markedly reduced compared with those from cells expressing Y27N or mock-transfected cells [Fig. 2*E*, VP1 (SUP)]. These results demonstrate that the interaction of agnoprotein and AP3D was necessary for the release of progeny virus.

We have demonstrated that agnoprotein binds to AP3D and suppresses AP-3–mediated vesicular trafficking and that the interaction of agnoprotein and AP3D is necessary for viroporin activity. Thus, there are two possible mechanisms to explain the regulation of viroporin activity. One is that a complex containing both agnoprotein and AP3D acts as a viroporin. The other is that agnoprotein inhibits AP-3 function and this leads to an enhancement of viroporin activity by agnoprotein itself. We used an siRNA against AP3D (siAP3D), which decreases both the interaction of agnoprotein with AP3D and AP-3 function. Cell membrane permeability for FM1-43FX dye with siAP3D was markedly increased compared with a negative control (siNC) in the presence of WT agnoprotein (Fig. 2*F*, *Left*). The increase of membrane permeability for FM1-43FX dye with siAP3D was also observed with the RK8AA mutant (Fig. 2*F*, *Right*), suggesting that the interaction of agnoprotein with AP3D is not necessary for viroporin function, but rather the inhibition of AP-3 function is important. Indeed, it could also be shown that knockdown of AP3D resulted in recovery of viroporin activity of the RK8AA mutant (Fig. S6 *A*–*D*).

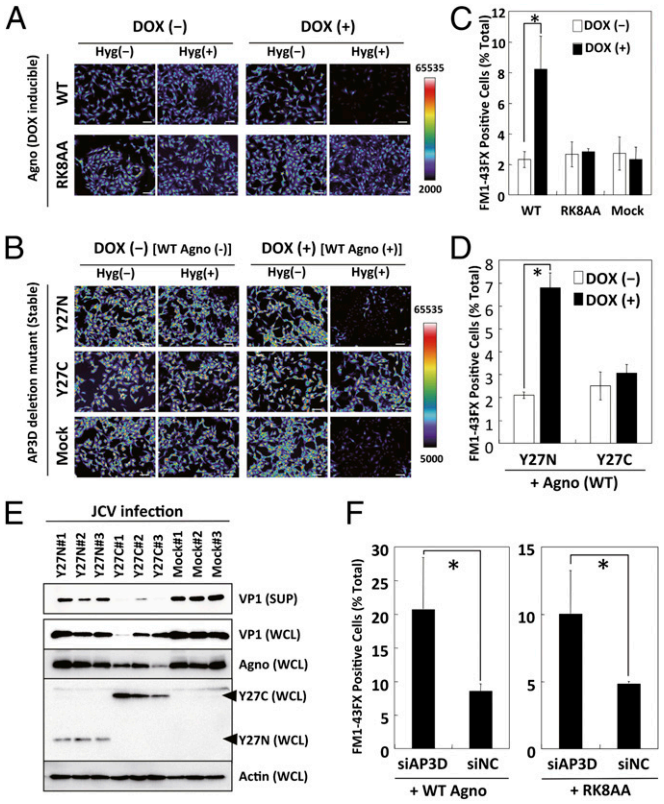

Fig. 2. Interaction of agnoprotein with AP3D is necessary for viroporin activity of agnoprotein. (*A*) SVG-AG cells (WT), which are wild type of agnoprotein-inducible cells with DOX treatment, or SVG-RK8AA cells (RK8AA), which are RK8AA mutant of agnoprotein-inducible cells with DOX treatment, were incubated with or without DOX. Nascent protein syntheses in these cells with or without HygB were labeled using the Click-iT AHA Alexa Fluor 488 Protein Synthesis Kit and observed by fluorescence microscopy. (Scale bars, 100 μm.) (*B*) SVG-AG cells stably expressing partial fragments of AP3D (Y27N or Y27C) or empty vector (Mock) were incubated with or without DOX. Nascent protein syntheses in these cells with or without HygB were labeled and observed by fluorescence microscopy. (Scale bars, 100 μm.) (*C*) SVG-AG cells (WT), SVG-RK8AA (RK8AA) cells, or SVG-Mock cells were incubated with or without DOX. Then the cells were stained with FM1-43FX dye. The cells were analyzed by flow cytometry. $*P < 0.05$. (*D*) SVG-AG cells stably expressing partial fragments of AP3D (Y27N or Y27C) were incubated with or without DOX, and then stained with FM1-43FX. $*P < 0.05$. (*E*) SVG-A cells stably expressing Myc-tagged AP3D-Y27N (Y27N) or Myc-tagged AP3D-Y27C (Y27C) or not expressing AP3D (Mock) were infected with JCV. These cells were harvested and lysed at 5 d after infection (WCL). Culture supernatants (SUP) of the cells were collected simultaneously and analyzed by immunoblotting with anti-VP1, anti-agnoprotein, anti-Myc antibody, or anti-actin antibodies. Arrowheads indicate the immunopositive signals of Y27C and Y27N. (*F*) SVG-AG cells (WT) and SVG-RK8AA cells (RK8AA) were transfected with siAP3D or siNC and incubated with DOX and then stained with FM1-43FX. $*P < 0.05$.

Inhibition of the AP-3 Pathway Enhances the Cell Surface Expression of Agnoprotein. Previously, we have shown that agnoprotein is in part cotranslationally inserted into the ER membrane and at later stages of infection transported to the plasma membrane. At the later stages, agnoprotein becomes more diffusely localized in the cytoplasm (3). When WT agnoprotein alone was expressed in glial cells, diffusely localized agnoprotein was observed in the cytoplasm in around 20% of cells. In contrast, the RK8AA mutant localized predominantly in the perinuclear region and did not exhibit such a diffuse pattern (Fig. S7 *A* and *B*). We performed flow cytometry analysis using anti-agnoprotein antibody on WT agnoprotein- or RK8AA mutant DOX-inducible cell lines. WT agnoprotein was evident on the cell surface at 48 h after DOX treatment. In contrast, the RK8AA mutant was poorly expressed on the cell surface (Fig. 3*A* and Fig. S7*C*), and overall, the expression on the cell surface was less than 30% of WT (Fig. S7*D*).

To investigate the role of AP-3 in the intracellular localization of agnoprotein, we performed immunofluorescence studies using SVG-AG or SVG-RK8AA cells. WT agnoprotein localized in the perinuclear region at 24 h after DOX treatment and then localized diffusely at 48 h (Fig. 3*B*, upper row). The RK8AA mutant localized in the perinuclear region similarly to WT at 24 h but then localized in granules in the cytoplasm at 48 h (Fig. 3*B*, lower row). The number of agnoprotein granules was significantly increased in RK8AA-expressing cells at 48 h and 72 h after DOX induction (Fig. 3*C*). Furthermore, the granules of RK8AA mutant, but not WT, were well colocalized with Lamp-2, the lysosomal marker protein (Fig. 3*D* and Fig. S8*A*).

We also performed immunofluorescence analysis of the WT and RK8AA agnoproteins following siAP3D knockdown. Diffusely localized agnoprotein was significantly higher with siAP3D treatment in both WT and RK8AA mutant agnoprotein-expressing cells (Fig. S8*B*). Furthermore, following siAP3D treatment, RK8AA was diffusely located in the cytoplasm but not corresponding with lysosomes (Fig. 3*E* and Fig. S8*C*). Meanwhile, not only RK8AA agnoprotein but also WT were expressed on the cell surface at higher levels in cells treated with siAP3D compared with siNC (Fig. 3*F*). These results show that disruption of AP-3 function by agnoprotein led to an increase in the expression of agnoprotein on the cell surface.

Agnoprotein Is Transported to the Lysosome for Degradation. Because the lysosomal degradation system would involve a reduction in the levels of transported proteins, we measured the effect of the inhibition of AP-3 on the cellular levels of agnoprotein. Total cellular levels of agnoprotein were seen to increase in a time-dependent manner following DOX treatment of SVG-AG cells transfected with siNC (Fig. S9*A*). In contrast, the levels of agnoprotein in cells with siAP3D quickly reached a maximum after induction with DOX (Fig. S9*A*), indicating that some of the agnoprotein was degraded by the pathway involving

the AP-3 complex. To determine the degradation rate of agnoprotein with AP3D knockdown, pulse–chase analyses using short periods of DOX treatment (8 h) on SVG-AG cells were performed (Fig. 4*A*). The levels of agnoprotein were seen to decrease in a time-dependent manner following washing out of DOX (DOX w/o) in cells transfected with siNC. In contrast, the levels of agnoprotein in cells with siAP3D were more stable (Fig. 4*A*), suggesting that the rate of degradation of agnoprotein was markedly reduced with the inhibition of AP-3 pathway.

To determine the degradation rate of agnoprotein with lysosomal protease inhibitor (LPI) (leupeptin, pepstatin A, and E64d) (23) treatment, pulse–chase analyses using DOX treatment of SVG-AG cells were performed (Fig. 4*B*). The levels of agnoprotein were seen to decrease in a time-dependent manner following DOX w/o in cells without LPI. In contrast, the levels of agnoprotein in cells with LPI were more stable (Fig. 4*B*), suggesting that the rate of degradation of agnoprotein was markedly reduced with inhibition of lysosomal degradation pathway. Furthermore, treatment with LPI led to the colocalization of both the WT and RK8AA mutant of agnoprotein with the lysosomal marker, Lamp-2 (Fig. 4*C* and Fig. S9*B*), suggesting that lysosomes can carry both the WT and RK8AA mutant of agnoprotein. These studies show that agnoprotein is transported and degraded in lysosomes in an AP-3–dependent mechanism.

On the basis of our findings, we propose a mechanism to outline the function of agnoprotein in virion release (Fig. 4*D*). Both WT and RK8AA agnoprotein form homooligomers as integral membrane proteins in the cytoplasmic organelles. WT agnoprotein specifically binds to AP3D and disrupts AP-3–mediated vesicular trafficking, preventing targeting to the lysosomal degradation pathway, which instead leads to translocation to the plasma membrane. In contrast, RK8AA mutant fails to effectively bind to the AP-3 complex δ subunit and to disrupt AP-3–mediated vesicular trafficking. This is instead transported to the lysosomes with subsequent lysosomal degradation. Consequently, WT agnoprotein, but not RK8AA mutant, enhances plasma membrane permeability and promotes virion release.

Discussion

Viroporins are small hydrophobic transmembrane proteins that interact with membranes modifying their permeability to ions and other small molecules. Viroporins form hydrophilic pores in the lipid bilayers and this can promote release of progeny virions from infected cells (6, 24). Some viroporins also have been shown to interfere with the intracellular vesicular trafficking pathways (16–19). However, the relationship(s) if any, between trafficking and viroporin activity remain unclear.

From our results, we consider that there may be at least three distinct populations of agnoprotein; the first directly binds to AP3D and inhibits AP-3 function; a second population is translocated to lysosomes dependent on AP-3 but without binding with AP3D, and this is degraded by lysosomal enzymes; and a third population reaches the plasma membrane to function as an oligomeric viroporin under conditions of a decline of AP-3 function.

In relation to the first population, we demonstrated that WT agnoprotein directly binds to AP3D, and this binding capacity was lost in the RK8AA mutant agnoprotein. We also demonstrated that WT agnoprotein inhibits AP-3 function, but RK8AA does not. These results suggest that WT agnoprotein inhibits AP-3 function by direct binding with AP3D (Fig. 1).

For the second population, the RK8AA mutant was detected in the perinuclear region similarly to WT agnoprotein and then localized in lysosomes at 48 h after induction. As the lysosomal localization of the RK8AA mutant was inhibited by siAP3D, the translocation to lysosome of RK8AA was dependent on AP-3–mediated vesicular trafficking (Fig. 3). Furthermore, minor populations of WT agnoprotein, which was only detected in the presence of a lysosomal protease inhibitor, were also transported and degraded in lysosomes in an AP-3–dependent mechanism (Fig. 4). This suggests that both WT and RK8AA agnoprotein were transported and degraded in lysosomes in an AP-3–dependent manner without direct binding of agnoprotein to AP3D. (This second population of WT agnoprotein is significantly smaller than that of RK8AA agnoprotein.)

Regarding the third population, agnoprotein in JCV-infected cells and DOX-inducible cell lines localized in the ER initially,

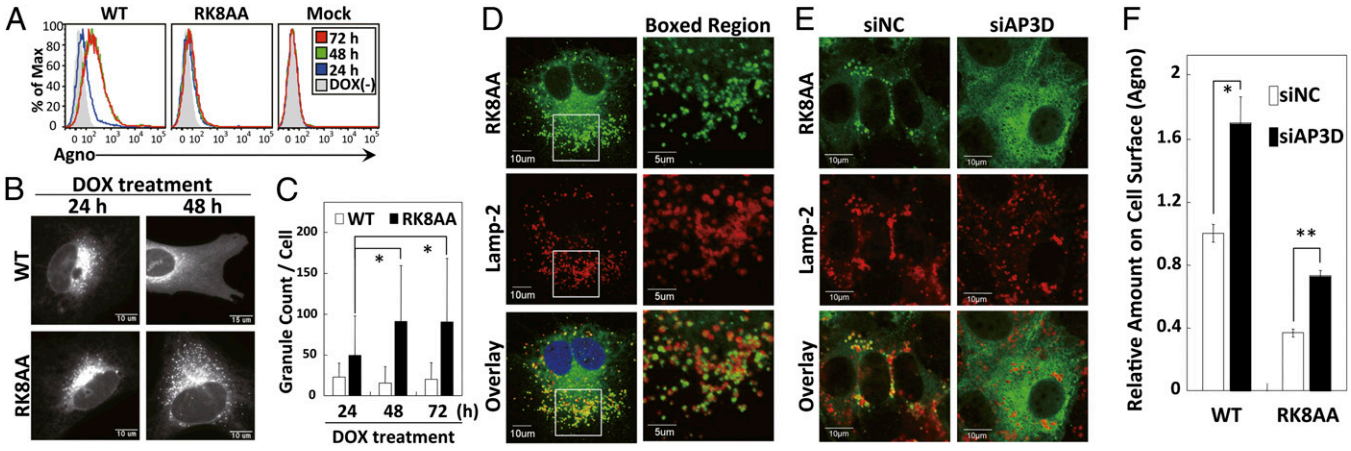

Fig. 3. Inhibition of AP-3 function is necessary for expression of agnoprotein on the cell surface. (*A*) SVG-AG cells (WT), SVG-RK8AA cells (RK8AA), or SVG-Mock cells (Mock) were incubated with or without DOX for indicated time points. The cells were subjected to cell surface staining using anti-agnoprotein antibody followed by Alexa Fluor 488-conjugated anti-rabbit IgG antibody and then analyzed by flow cytometry. (*B* and *C*) SVG-AG cells (WT) or SVG-RK8AA cells (RK8AA) were incubated with DOX for the indicated time. The cells were subjected to immunofluorescence analysis using anti-agnoprotein antibody followed by Alexa Fluor 488-conjugated anti-rabbit IgG antibody. We observed agnoprotein-positive granules. The granular localization of agnoprotein was quantified by MetaMorph software at the indicated time points. (Scale bars, 10 or 15 μm.) (*C*) The bar graph indicates the average granular localization of agnoprotein in a single cell. Results are average of three independent experiments. $*P < 0.05$. (*D*) Confocal microscopy analysis of SVG-RK8AA cells showed the colocalization of RK8AA mutant of agnoprotein with Lamp-2, the lysosome marker. The boxed areas in the left column are shown at higher magnification in the right column. [Scale bars, 10 μm (left column) and 5 μm (right column).] (*E*) SVG-RK8AA (RK8AA) cells were transfected with siAP3D or siNC and incubated with DOX. The cells were subjected to confocal microscopy analysis. The colocalization of RK8AA with Lamp-2 was decreased in the cells transfected with siAP3D compared with those transfected with siNC. (Scale bars, 10 μm.) (*F*) SVG-AG cells (WT) or SVG-RK8AA cells (RK8AA) transfected with siAP3D or siNC were incubated with DOX. The levels of agnoprotein expression on cell surface were measured by flow cytometry using Alexa Fluor 647-labeled anti-agnoprotein antibody. The bar graph indicates the relative mean fluorescence intensity of agnoprotein ($*P < 0.05$ and $**P < 0.01$).

and was then transported to the plasma membrane at later stages of infection (Fig. 3). The signal sequence-dependent protein sorting usually occurs soon after translation without a significant time lag. However, agnoprotein was not transported to the cell surface immediately after translation, suggesting that transport of agnoprotein to the cell surface may not depend on the signal sequences of agnoprotein. In AP-3 complex-deficient mammalian cells, it has been reported that some lysosomal membrane proteins were missorted to the plasma membrane (20, 21). WT agnoprotein inhibited AP-3–mediated transport of the lysosomal membrane protein to lysosomes and increased the expression of the protein on cell surface, and WT and RK8AA mutant agnoprotein were transported to the cell surface following knockdown of AP3D expression. Taken together, cellular surface expression of agnoprotein is dependent on inhibition of AP-3 function. We suggest that the second population of WT agnoprotein is decreased by the AP-3 inhibitory effect of the first population of agnoprotein, resulting in increases in the third population of WT agnoprotein.

In summary, our studies demonstrate that agnoprotein specifically binds to and disrupts AP-3–mediated vesicular trafficking, preventing targeting to the lysosomal degradation pathway and which instead leads to translocation to the plasma membrane with resulting membrane permeabilization. Further investigations are required to determine if the viroporins of other viruses might likewise be highly regulated.

Materials and Methods

Detailed methods are provided in *SI Materials and Methods*. These describe viruses, transfections, immunoprecipitation assays, GST pull-down assay, immunofluorescent staining, flow cytometry, details of antibodies and other reagents, and statistical methods.

JCV Growth/Genome Transfection Assay. SVG-A cells stably expressing myc-tagged AP3D-Y27N or AP3D-Y27C were grown to 50% confluence on a six-well plate and incubated with 1,000 HA units of JCV. The whole-cell lysates (WCLs) and culture supernatants were harvested and analyzed by immunoblot analysis at indicated times after infection. For JCV genome transfection assays, mutant and WT viral DNA were linearized at the Bam HI site, and equal amounts of viral DNA were transfected into permissive SVG-A cells by Fugene HD (Roche Diagnostics) reagents according to the manufacturer's instructions. For quantification of viral particle release, the culture supernatant was collected at indicated times after transfection and ultracentrifuged in a Beckman TLA-100.3 rotor at 80,000 rpm for 60 min at 4 °C. The pellet fraction and WCLs were analyzed simultaneously by immunoblotting. Results were confirmed by at least three independent experiments.

VSVG-GFP Transport Assay. The 293T or 293AG cells with or without DOX (50% confluent) grown on 35-mm glass-bottomed dishes were transiently transfected using FuGENE 6 (Roche Diagnostics) with pVSVG-GFP. Transfection was performed according to the manufacturer's instructions. After transfection, the cells were incubated at 39.5 °C for 20 h. Before a temperature shift from 39.5 °C to either 20 °C or 32 °C, 20 μg/mL of cycloheximide was added to each dish. The cells were fixed at the indicated time points and then processed for confocal fluorescence microscopy (Olympus).

Membrane Permeability Assay. Permeability of the plasma membranes to Hygromycin B (HygB) was determined using the Click-iT L-azidohomoalanine (AHA) Alexa Fluor 488 Protein Synthesis HCS Assay kit (Invitrogen) with slight modification. Click-iT AHA is an amino acid analog of methionine containing an azide moiety. Similar to [^{35}S]methionine, Click-iT AHA is added to cultured cells, and the amino acid is incorporated into proteins during active protein synthesis. Detection of the incorporated amino acid uses a chemoselective ligation or click reaction between an azide and alkyne, where the azido-modified protein is detected with an Alexa Fluor 488 alkyne. DOX-inducible agnoprotein-expressing cells were seeded in 96-well plates with or without DOX. After 72 h incubation, the cells were incubated in L-methionine and L-cystine–free DMEM (Invitrogen) supplemented to contain 200 μM L-cystine, 2 mM L-glutamine, and 10 mM Hepes for 1 h. Then, the cells were incubated for 1 h in 100 μM Click-iT AHA containing medium with or without 500 μg/mL HygB. Detection of Click-iT AHA incorporation into nascent synthesized protein was assayed with the Click-iT AHA Alexa Fluor 488 Protein Synthesis HCS Assay kit according to the manufacturers' protocols. The cells were imaged as previously described. Nuclei were labeled with Hoechst 33342 solution, and the cells were imaged with an inverted fluorescence/phase-contrast microscopy (Olympus) equipped with cooled CCD camera (Olympus). The fluorescence intensity of Alexa Fluor 488 corresponding to nascent protein syntheses in single cells was analyzed using Cell Scoring Application Module of MetaMorph software. The bar graph indicates the proportion of mean signal intensity of Alexa Fluor 488 of the cells in the presence of HygB compared with those in the absence of HygB. The measurement of HygB permeability shown in Fig. S6C was previously described (3). For evaluation of membrane permeability to the lipophilic dye FM1-43FX (Invitrogen), DOX-inducible agnoprotein-expressing cells were incubated with or without

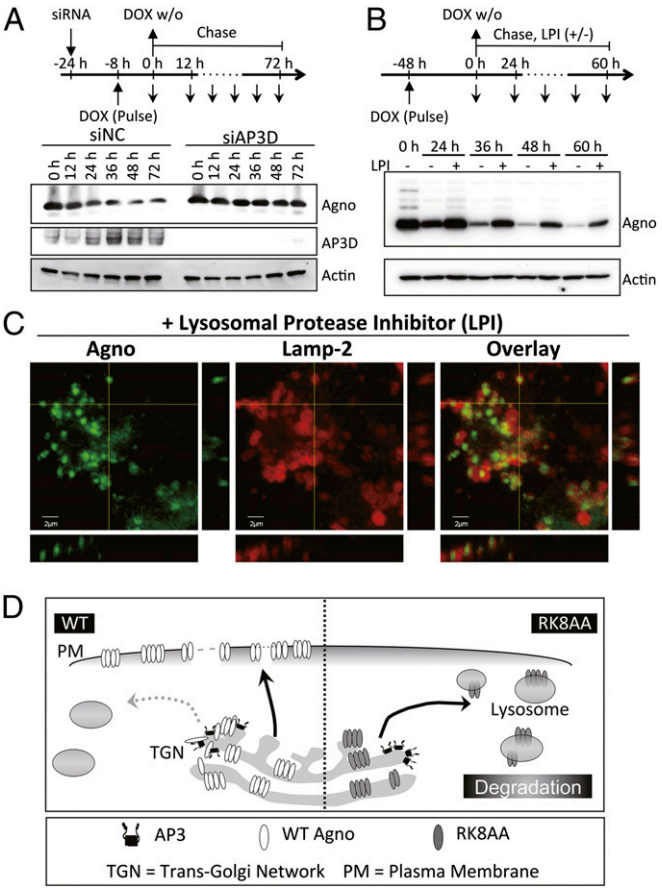

Fig. 4. AP-3–mediated vesicular trafficking transports agnoprotein to the lysosome for degradation. (*A*) Pulse–chase experiments using short period of DOX treatment. SVG-AG cells were transfected with siAP3D or siNC (−24 h), and then the cells were treated with DOX for 8 h following PBS washing and changing the medium without DOX (0 h). The cell lysates were collected at the indicated time and subjected to immunoblotting using anti-AP3D, anti-actin, and anti-agnoprotein antibodies. (*B*) SVG-AG cells were treated with DOX for 48 h following PBS washing and changing the medium without DOX (0 h). Then the cells were incubated with or without a mixture of LPI (containing 40 μM leupeptin, 40 μM pepstatin A, and 4 μg/mL E64d) for the indicated time and subjected to immunoblotting. (*C*) DOX-treated SVG-AG cells were cultured in the presence of a mixture of lysosome protease inhibitors (LPI) for 48 h. The cells were processed for immunofluorescence staining for agnoprotein and a lysosome marker Lamp-2 and analyzed by confocal microscopy. *Z*-section images were also acquired on a confocal microscopy. (Scale bars, 2 μm.) (*D*) A model to illustrate the involvement of AP-3 in membrane permeabilization and virion release. The left and right sides of the schematic representation shows events with the WT agnoprotein and the RK8AA mutant, respectively. Both WT and RK8AA form homooligomers as integral membrane proteins in cytoplasmic organelles. WT disrupts AP-3–mediated vesicular trafficking, is translocated to plasma membrane, and functions as a viroporin, resulting in the promotion of virion release. In contrast, the RK8AA mutant, which fails to bind to AP3D and to disrupt AP-3–mediated vesicular trafficking, is transported to lysosomes and degraded. Consequently, RK8AA cannot promote virion release and is defective in viral propagation.

1 μg/mL DOX for 72 h. The cells were stained with FM1-43FX dye in HBSS without magnesium or calcium on ice for 1 min to slow down endocytosis. The cells were then washed with ice-cold PBS and fixed for 30 min in ice-cold 4% (wt/vol) paraformaldehyde (PFA)/PBS. The washing step removes the dye from the plasma membrane, whereas FM1-43FX stained in the intracellular compartments is retained and can be fixed. Cells were imaged as previously described. For flow cytometry of the cells stained with FM1-43 FX dye, the cells were detached using an enzyme-free/PBS-based cell dissociation buffer (Invitrogen) according to the manufacturer's instructions and then stained. The cells were fixed for 30 min in ice-cold 4% (wt/vol) PFA/PBS and analyzed by FACScanto (BD Bioscience).

ACKNOWLEDGMENTS. We thank Dr. K. Tokunaga for valuable suggestions on immunofluorescence analysis with lysosomal protease inhibitors and Ms. S. Yamanouchi for excellent technical assistance. This study was supported in part by grants from the Ministry of Education, Culture, Sports, Science, and Technology (MEXT); the Ministry of Health, Labor, and Welfare; and the Program of Founding Research Centers for Emerging and Reemerging Infectious Diseases, MEXT.

1. Hirsch HH, Kardas P, Kranz D, Leboeuf C (2013) The human JC polyomavirus (JCPyV): Virological background and clinical implications. *APMIS* 121(8):685–727.
2. Ferenczy MW, et al. (2012) Molecular biology, epidemiology, and pathogenesis of progressive multifocal leukoencephalopathy, the JC virus-induced demyelinating disease of the human brain. *Clin Microbiol Rev* 25(3):471–506.
3. Suzuki T, et al. (2010) The human polyoma JC virus agnoprotein acts as a viroporin. *PLoS Pathog* 6(3):e1000801.
4. Nieva JL, Madan V, Carrasco L (2012) Viroporins: Structure and biological functions. *Nat Rev Microbiol* 10(8):563–574.
5. Montserret R, et al. (2010) NMR structure and ion channel activity of the p7 protein from hepatitis C virus. *J Biol Chem* 285(41):31446–31461.
6. Gonzalez ME, Carrasco L (2003) Viroporins. *FEBS Lett* 552(1):28–34.
7. Agirre A, Barco A, Carrasco L, Nieva JL (2002) Viroporin-mediated membrane permeabilization. Pore formation by nonstructural poliovirus 2B protein. *J Biol Chem* 277(43):40434–40441.
8. Melton JV, et al. (2002) Alphavirus 6K proteins form ion channels. *J Biol Chem* 277(49): 46923–46931.
9. Pavlović D, et al. (2003) The hepatitis C virus p7 protein forms an ion channel that is inhibited by long-alkyl-chain iminosugar derivatives. *Proc Natl Acad Sci USA* 100(10):6104–6108.
10. Han Z, Harty RN (2004) The NS3 protein of bluetongue virus exhibits viroporin-like properties. *J Biol Chem* 279(41):43092–43097.
11. Wilson L, McKinlay C, Gage P, Ewart G (2004) SARS coronavirus E protein forms cation-selective ion channels. *Virology* 330(1):322–331.
12. Ito M, Yanagi Y, Ichinohe T (2012) Encephalomyocarditis virus viroporin 2B activates NLRP3 inflammasome. *PLoS Pathog* 8(8):e1002857.
13. Hyser JM, Collinson-Pautz MR, Utama B, Estes MK (2010) Rotavirus disrupts calcium homeostasis by NSP4 viroporin activity. *mBio* 1(5):e00265-10.
14. DeDiego ML, et al. (2007) A severe acute respiratory syndrome coronavirus that lacks the E gene is attenuated in vitro and in vivo. *J Virol* 81(4):1701–1713.
15. Kuo L, Masters PS (2003) The small envelope protein E is not essential for murine coronavirus replication. *J Virol* 77(8):4597–4608.
16. Deitz SB, Dodd DA, Cooper S, Parham P, Kirkegaard K (2000) MHC I-dependent antigen presentation is inhibited by poliovirus protein 3A. *Proc Natl Acad Sci USA* 97(25): 13790–13795.
17. Dodd DA, Giddings TH, Jr., Kirkegaard K (2001) Poliovirus 3A protein limits interleukin-6 (IL-6), IL-8, and beta interferon secretion during viral infection. *J Virol* 75(17):8158–8165.
18. de Jong AS, et al. (2006) The coxsackievirus 2B protein increases efflux of ions from the endoplasmic reticulum and Golgi, thereby inhibiting protein trafficking through the Golgi. *J Biol Chem* 281(20):14144–14150.
19. Cornell CT, Kiosses WB, Harkins S, Whitton JL (2006) Inhibition of protein trafficking by coxsackievirus b3: Multiple viral proteins target a single organelle. *J Virol* 80(13):6637–6647.
20. Robinson MS, Bonifacino JS (2001) Adaptor-related proteins. *Curr Opin Cell Biol* 13(4): 444–453.
21. Lefrançois S, Janvier K, Boehm M, Ooi CE, Bonifacino JS (2004) An ear-core interaction regulates the recruitment of the AP-3 complex to membranes. *Dev Cell* 7(4):619–625.
22. Nishimura N, Plutner H, Hahn K, Balch WE (2002) The delta subunit of AP-3 is required for efficient transport of VSV-G from the trans-Golgi network to the cell surface. *Proc Natl Acad Sci USA* 99(10):6755–6760.
23. Iwabu Y, et al. (2009) HIV-1 accessory protein Vpu internalizes cell-surface BST-2/tetherin through transmembrane interactions leading to lysosomes. *J Biol Chem* 284(50):35060–35072.
24. Raghava S, Giorda KM, Romano FB, Heuck AP, Hebert DN (2013) SV40 late protein VP4 forms toroidal pores to disrupt membranes for viral release. *Biochemistry* 52(22): 3939–3948.